A new PET insert for simultaneous PET/MR small animal imaging

Hans F Wehrl[1], Konrad Lankes[1,2], Mosaddek Hossain[1], Ilja Bezrukov[1,3], Chih-Chieh Liu[1], Petros Martirosian[4], Gerald Reischl[1], Fritz Schick[4], and Bernd J Pichler[1]
[1]Department for Preclinical Imaging and Radiopharmacy, University of Tuebingen, Tuebingen, Germany, [2]Bruker BioSpin MRI, Ettlingen, Germany, [3]Max Planck Institute for Intelligent Systems, Tuebingen, Germany, [4]Section on Experimental Radiology, University of Tuebingen, Tuebingen, Germany

Introduction:

Combined, simultaneous PET and MR imaging in small animals is a excellent research tool, allowing monitoring of metabolic processes on multiple levels. However the first generation of these imaging devices has suffered from some drawbacks in terms of PET and MR performance, as well as limited field of view, compared to the respective stand alone solutions. Here we present a new design of a high efficiency, small animal, PET/MR system allowing for studies of rats and mice. PET and MR performance have been extensively assessed. In vivo studies are presented that show the potential of PET/MR techniques in small animal research.

Material and Methods:

PET/MR System: The PET insert consists of 16 detector cassettes, each featuring three Lutetium oxyorthosilicate (LSO) crystal blocks (15x15 crystals per block, 1.5x1.5x10mm³) mounted along the z-direction (Figure 1). The LSO crystals are coupled via a small light guide to a 3x3 Avalanche Photodiode (APD) array, allowing for a MR compatible signal detection. In addition to a whole body RF coil multi-channel local RF coils can be used inside the PET-insert. The combined PET/MR FOV is 72mm in transversal as well as 72mm in axial direction. The PET insert is installed inside a 7T small animal MR scanner (Bruker/Siemens ClinScan).

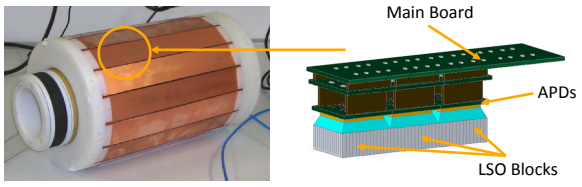

Figure 1: a) view of the PET insert with a whole body coil installed, the inner diameter with MR coil is 72 mm. b) a single PET detector module is shown, with the MR compatible LSO crystal blocks coupled to APDs.

PET Performance: Spatial resolution: A 22mm long glass capillary tube, with a volume of 10µL was filled with 1MBq of [^{18}F]FDG solution and positioned at the center of the combined PET/MR FOV. Different PET reconstruction algorithms (FBP2D, OSEM2D with 4 and 16 iterations) as well as measurements without and with MR sequence (GRE EPI, TR=2000ms, TE=18ms) running were performed. Sensitivity: The sensitivity of the PET-insert was assessed using a 10mm sphere filled with 340kBq of [^{18}F], and an energy window of 350-650keV.

MR Performance: MR performance in terms of signal-to-noise-ratio (SNR) as well as image homogeneity was measured without and with the PET insert installed. The temporal stability of the MR system was studied adhering to a modified fBIRN EPI stability protocol.

In vivo imaging: To study the in vivo imaging capabilities of this new PET/MR system, two animal studies were performed. In a first study Balb/c mice (n=3) bearing a *s.c.* CT26 tumor were *i.v.* injected with 26kBq [^{18}F]fluoroazomycin arabinoside ([^{18}F]FAZA), a PET tracer for tumor hypoxia. For MRI a breathing challenge, consisting of up to three air-carbogen cycles (each lasting for 5min) was applied for the duration of a segmented EPI sequence (TR=880ms/15s (effective), TE=8.1ms). Hypoxic tumor regions imaged by [^{18}F]FAZA PET as well as significantly responding regions in the MRI were identified and compared. In a second study, 18kBq of [^{18}F]FDG were *i.v.* injected in rats, and simultaneous cardiac imaging using PET/MR was performed.

Results:

PET Performance: The spatial resolution (n=3) of the PET-insert in transaxial direction was assessed (without/with MR sequence) for FBP: (2.58±0.05/2.60±0.05)mm, OSEM2D 4iter: (2.26±0.06/2.19±0.05)mm, and OSEM 2D 16iter: (2.22±0.10/2.18±0.14)mm and in axial direction for FBP: (2.80±0.09/2.96±0.09)mm, OSEM2D 4iter: (2.56±0.10/2.61±0.13)mm, and OSEM 2D 16iter: (2.45±0.13/2.59±0.09)mm. The sensitivity of the PET insert without running MR sequence at the center of the FOV (3.19±0.22)% was not significantly different from the measurement with MR sequence (3.10±0.08)%.

MR Performance: The results of the SNR and image homogeneity measurements (n=18) are given in Figure 2. Only for the TSE sequence a small (2%), but significant ($p<0.05$) decrease in SNR and image homogeneity could be observed. For the other sequences no significant change in SNR and image homogeneity due to the presence of the PET insert was observed. The EPI temporal stability (n=3) showed no significant changes (without/with PET insert) of the signal drift (0.6±0.2/0.4±0.1)% and the root-mean-square stability (0.125±0.003/0.166±0.040)%.

In vivo imaging: Hypoxia-study: Complementarities between the areas of high [^{18}F]FAZA uptake and areas significantly ($p<0.05$) responding to breathing challenges within the CT-26 tumors are observed (Figure 3). In addition excellent identification of anatomical details and uptake areas is possible by combined PET/MR imaging. BOLD signal changes due to the breathing challenge are in the order of ±3.3%. Cardiac-imaging: Gated MR and PET images with high image quality were acquired. A clear delineation of the cardiac ventricles was possible in MR as well as PET (Figure 4).

Discussion and Conclusions:

The PET insert performance in the combined PET/MR system is in the same range as a commercially available stand alone PET scanner. The PET spatial resolution of 2.2mm in the center FOV can be improved by a reconstruction method adapted specifically to the PET insert. The slight drops in SNR and image homogeneity for the TSE sequence are caused by small deviations from repositioning. The temporal stability of the MR system allows obtaining fMRI data in the presence of the PET insert. The simultaneous hypoxia imaging study, using [^{18}F]FAZA PET and BOLD imaging revealed that both methods can be applied complementary. Tumor areas showing significant signal change during breathing challenges were marked by a low [^{18}F]FAZA uptake in the PET and vice versa. Subtle differences could be due to [^{18}F]FAZA PET revealing intracellular hypoxia whereas the non responding BOLD areas correspond to extracellular hypoxia. The high resolution cardiac imaging study showed that the heart also can be imaged by simultaneous PET/MR. In summary, we have presented a new generation of a small animal PET insert that is capable to deliver an image quality on par with stand alone PET systems. In addition the in vivo study examples reveal the multitude of metabolically processes that can be studied with this new technology.

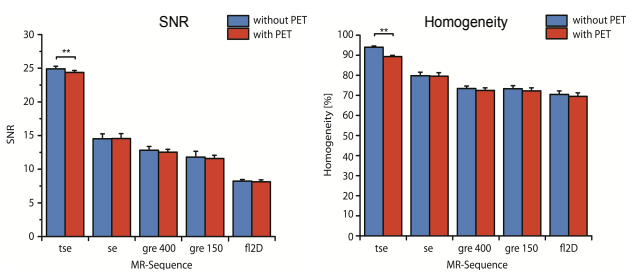

Figure 2: MR signal-to-noise ratio (SNR) and image homogeneity assessed without and with the PET insert installed and running.

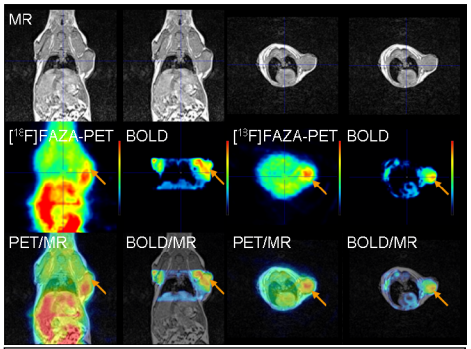

Figure 3: PET/MR tumor hypoxia imaging shows complementarities of both methods in some areas.

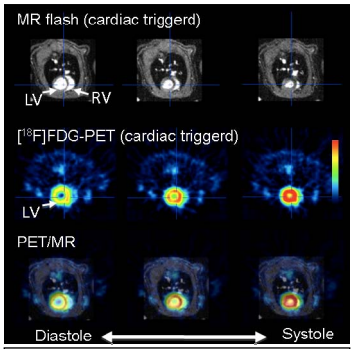

Figure 4: Cardiac imaging of a rat using combined, simultaneous PET/MR.